

# Reconstruction of Tomographic Size Using a Filtered Back Projection Algorithm

**FAIEZ MUSA LAHMOOD ALRUFAYE, SEHAM AHMED HASHEM**

Middle Technical University, Baghdad, Iraq

Corresponding author: Faiez Musa Lahmood Alrufaye (e-mail: [Faiez.Alrufaye@mtu.edu.iq](mailto:Faiez.Alrufaye@mtu.edu.iq)).

**ABSTRACT** Due to their widespread use, image processors are among the most essential computer processors. FBP technique is one of the most widely used tomographic reconstruction methods. Images from a computed tomography (CT) scanner with 512x512 pixels of raw data for parallel beam projections are the metadata to which this approach is applied. This work is divided into three parts. Several projections are created from an input test picture termed Shepp-Logan phantom in the first section, utilizing radon transformation. The picture is rebuilt from the projection of a parallel beam in the second section to minimize reconstruction time. Finally, the proposed system filters the projections using the Ram Lak filter and the Hann window in the third section to refine the picture and then recombine the projections to generate the reconstructed image. The reconstruction procedure is performed on CT images using a filtered back-projection algorithm in this article for image optimization and then projection recombination to generate the rebuilt picture. Since CT can accurately depict anatomical elements like bones and organs and may pick slides in any orientation, it is frequently used in biological applications and diagnostics. It also offers a great spatial resolution and soft tissue contrast. We develop, create, and run computer programs when we work with MATLAB. After projecting the 2D image onto a CT scanner, a very good result in reconstructing the image is received.

**KEYWORDS** Filtered Back Projection; FBP; Computerized Tomography; Sinogram; Head Phantom.

## I. INTRODUCTION

BECAUSE computer technologies provide simple access to precise and quick findings, they have become commonplace in almost every aspect of life. Image processing technology is the most essential of these approaches. Image processing is divided into two stages: the image analysis stage, in which the image is analyzed to obtain its features, which will be used later in the stage; and the post-analysis stage, in which the image is analyzed to obtain its features, which will be used later in the post-analysis stage. The building or reconstruction step is the second stage of image processing; in this stage, the picture is recreated using the features retrieved in the first stage (the image analysis stage). The goal of this stage is to rebuild the image in order to enhance its quality and accuracy.

The filtered back projection algorithm (FBP) is a commonly used method for reconstructing tomographic images. This method was utilized on a computerized tomography (CT) scanner. The use of a 512 x 512 pixel CT image reconstruction method from raw data for parallel beam projections is presented in this study. This work is divided into three sections. In the first stage, the Radon transform is used to generate a large number of projections from the input test picture known as the Shepp-Logan phantom. In the second stage, parallel beam

projection is used to rebuild the image, which shortens the reconstruction time. The reconstructed picture is produced in the third section by using back projection summation and the Hann window and Ram Lak filter to filter the projections for image improvement [1].

Similar to how the distribution function establishes the density distribution of a region explored using projections, the Austrian Mathematician Radon proposed a procedure for reconstructing an object using the resulting projections in 1971. In the medical area, EMI Ltd. presented the first commercial computerized X-ray tomography in 1973 [1]. On the other hand, Cormack proposed an array of slice part-related coefficients that could be obtained by transmitting X-rays across an object at different angles and obtaining images of transverse parts [3]. Cormack also demonstrated a mathematical method for reconstructing images using a finite number of projections [2].

The item's internal features will be examined using a computerized Tomography scanner (CT). Table 1 [4] lists the CT scanner generations. The main system consists of a computer system, gantry, control panel, and patient table. The gantry contains the data-acquisition system (DAS), x-ray detectors, and x-ray source [5].

**Table 1. Scanner generations of CT**

Scanner Generation	Scanner Description
1 <sup>st</sup> generation	Translate-rotate motion, or the first generation scanner, combines incremental rotation with linear translation.
2 <sup>nd</sup> generation	Multiple narrow rays are used in the second generation of CT, which employs single-source tomography and multiple detectors. Translation-rotation is the name of the scanner movement.
3 <sup>rd</sup> generation	The detector group is tightly coupled to an X-ray tube in third-generation CT scanners, allowing the tube and detectors to rotate around the body simultaneously (movement is referred to as the rotational motion).
4 <sup>th</sup> generation	The body is circled by an X-ray tube alone in the fourth generation CT scanner, which incorporates a sizable fixed loop of chemicals.
5 <sup>th</sup> generation	A fifth generation CT scanner is one that has numerous rows of detectors and many slices.

## II. RELATED WORKS

There has been a lot of research that has addressed and used the filtered back projection technique; in this section of the study, we will analyze some of the research works and compare the findings with the proposed system.

Data-parallel tomographic reconstruction was utilized by Jos B.T.M. Roerdink and Michel A. Westenberg, who compared filtered back projection with direct Fourier reconstruction. These algorithms run on a Connection Machine CM-5, which has 16 processors and a max speed of 2 Gflop/s [5].

Researchers Samit BasuYoram and Bresler Yoram proposed a novel parallel-beam CT rapid reconstruction approach. The new approach is a faster variant of the traditional filtered back projection (FBP) reconstruction, which employed a hierarchical back projection decomposition to reduce the cost from  $O(N_3)$  to  $O(N_2)$  ( $N_2 \log 2$ ). They addressed the effects of various parameter choices on algorithm behavior and gave numerical simulations that demonstrated the cost versus distortion tradeoff [6].

A comprehensive cost and algorithm performance analysis was conducted on a general-purpose platform by Thammanit Pipatsrisawat, Aca Gacic, Franz Franchetti, Markus Puschel, and Jose M. F. Moura. They examined the tradeoffs between distortion and runtime by adjusting various algorithm and implementation variables using precisely calibrated implementations of both the direct and hierarchical back projections [7].

Marwa T. Al Hussani and Mohammed H. Ali Al Hayani reported their development of a 512X512 pixel tomographic reconstruction technique from the raw data of parallel beam projections in 2014. They were able to rebuild a 2D picture after projecting it into a CT scanner with excellent results [8].

Nikolay Koshev, Elias S. Helou, and Eduardo X. Miqueles suggested a novel rapid back projection operator [9] in 2018 for processing tomographic data and compared it to previous fast reconstruction approaches.

For a generated image of the object, Tuba Zge Onur provided a reconstruction approach using the Filtered Back Projection (FBP) algorithm. Performance enhancement was observed after forming the filtered back projection image with

the Shepp-Logan filter. The produced images suggested that the FBP algorithm could be useful for a number of applications in the fields of industry and medicine [10].

Kyuhyouon Cho and colleagues proposed the method, which resulted in a revised sinogram, resolved the blocking issue. The revised sinogram (SDO) was produced by combining the EUV data acquired by the Atmospheric Imaging Assembly on board the Solar Dynamics Observatory at two distinct locations. In February 2019, they produced the modified sinogram for about a month and, using the static state hypothesis, rebuilt the three-dimensional corona. Using a differential emission measure inversion technique, scientists were able to determine the corona's physical properties. They assessed the efficacy of the FBP approach with the revised sinogram by contrasting the reconstructed data with the observed EUV picture, electron density models, previous studies of electron temperature, and an observed coronagraph image. The results showed how well the FBP algorithm could replicate the physical characteristics of the coronal holes and dazzling spots. The FBP algorithm's key benefits are that it is simple to grasp and computationally effective. As a result, it made it simple for them to investigate the solar corona's uneven temperature and coronal electron density [11].

We developed a method to rebuild pictures using a filtered back projection technique and tested it on CT scans as part of our study.

## III. ALGORITHM FOR FILTERED BACK PROJECTION

Using a set of projections called  $p(t, \theta)$ , image reconstruction is the process of anticipating an object image slice from  $f(x, y)$ . There are numerous methods that can be used to complete this work, each of which has advantages of its own [12].

The mathematical toolkit for image reconstruction is built based on the reconstruction approach [13]. Using convolution and a one-dimensional integral equation, the FBP method reconstructs a two-dimensional picture. It is the most often utilized approach in CT applications [14].

In the Fourier slice theory, values of the item along a single line are obtained using a single projection and the two-dimensional (2D) Fourier transform [15].

Assuming that the remaining projections are all equal to zero, a simple reconstruction can be built by computing the two-dimensional inverse Fourier transform and positioning the transformation values for this projection in the proper locations within the two-dimensional Fourier domain of the object [17].

The algorithm for completely refined rear projection is as follows [18]:

- Each of the  $K$  angles  $\theta$  sum, between  $0^\circ$  and  $180^\circ$ ,
- Calculate the projection,  $P_\theta(t)$ ,
- Fourier transform it to discover  $S_\theta(r)$ ,
- It should be multiplied by the weighting factor ( $r$ )  $2\pi|r|/K$ ,
- Filtered projections above the picture plane with inverted Fourier transforms (back projection process).

By calling the two-dimensional formula the inverse Fourier transform, the object function  $f(x, y)$  can be written as follows [19]:

$$f(x, y) = \int_{-\infty}^{\infty} \int_{-\infty}^{\infty} F(m, n) e^{j2\pi(ux+vy)} dm dn. \quad (1)$$

In the frequency domain of a polar coordinate system, the rectangular coordinate system is exchanged by making substitutions [14]:

$$\begin{aligned} m &= r \cos \theta \\ n &= r \sin \theta \end{aligned} \quad (2)$$

The differentials are changed using:

$$dm dn = r dr d\theta. \quad (3)$$

A polar function's inverse Fourier transform can be expressed as:

$$\begin{aligned} f(x, y) &= \int_0^{2\pi} \int_0^{\infty} F(r, \theta) e^{j2\pi r(x \cos \theta + y \sin \theta)} r dr d\theta \\ &+ \int_0^{\pi} \int_0^{\infty} F(r, \theta + 180^\circ) e^{j2\pi r[x \cos(\theta + 180^\circ) + y \sin(\theta + 180^\circ)]} r dr d\theta \end{aligned} \quad (4)$$

After which system uses the property:

$$F(r, \theta + 180^\circ) = F(-r, \theta). \quad (5)$$

It is possible to write the above phrase as:

$$f(x, y) = \int_0^{\pi} \left[ \int_{-\infty}^{\infty} F(r, \theta) |r| e^{j2\pi r t} dr \right] d\theta. \quad (6)$$

By setting, we have simplified the expression:

$$t = x \cos \theta + y \sin \theta. \quad (7)$$

For the two-dimensional Fourier transform, we substitute the Fourier transform of the projection at angle  $\theta$ :

$$f(x, y) = \int_0^{\pi} \left[ \int_{-\infty}^{\infty} S_{\theta}(r) |r| e^{j2\pi r t} dr \right] d\theta. \quad (8)$$

This integral in the previous equation can be written as:

$$f(x, y) = \int_0^{\pi} Q_{\theta}(x \cos \theta + y \sin \theta) d\theta, \quad (9)$$

where

$$Q_{\theta}(t) = \int_{-\infty}^{\infty} S_{\theta}(r) |r| e^{j2\pi r t} dr. \quad (10)$$

Considering the projection data transformation, estimating  $f(x, y)$  is simple. The last equation, which gives the frequency response to the filter as  $|r|$ , represents the filtering process and is hence referred to as a "filtered projection." Addition of projections from various angles yields an estimate of  $f(x, y)$ , which may be expressed by an alternative approximation of the integral in (9):

$$f(x, y) = \frac{\pi}{K} \sum_{i=1}^k Q_{\theta_i}(x \cos \theta_i + y \sin \theta_i), \quad (11)$$

where the projections  $P_{\theta}(t)$  are those for which the  $K$  angles  $\theta_i$ .

#### IV. THE PROPOSED SYSTEM

A reverse projection filter method is used to rebuild an object from its projection. High-pass filters are used to filter projections in order to lessen the blurring effects of back projection and restore object clarity. The following actions are suggested in order for a computer model to replicate the entire process [20-22]:

- A parallel genogram (radon transformation) is created from two-dimensional pictures of 512 x 512 pixels.
- The fast Fourier transform (FFT) is applied to the radon transform's output matrix.
- A frequency-domain slope filter is multiplied by the Hann window in the projection filter. To minimize excessive noise amplification at these frequencies, picture reconstruction frequently employs a limited-band filter known as the Ram-Lak filter.
- Use posterior projection as back staining, which involves obtaining a radial sample at each angle and staining it along the path we have integrated, in order to precisely weight ( $r$ ) the projections.

In order to enhance the functionality of the FBP algorithm, we present a method for picture reconstruction of a head ghost. The MATLAB software was used as a useful programming tool for the proposed reconstruction. Data from DAS were gathered by scanning parallel beam geometry with MATLAB functions on the 512 512-pixel image provided for reconstruction as a head phantom test image, as illustrated in Figure 1 [23, 24]. This metadata will be filtered away by multiplying the Ram-Lak filter by a window. Estimated Reconstruction Time for the Han window is enhanced. The reconstruction mechanism is depicted in Figure 2 as a block diagram.



Figure 1. Phantom head input

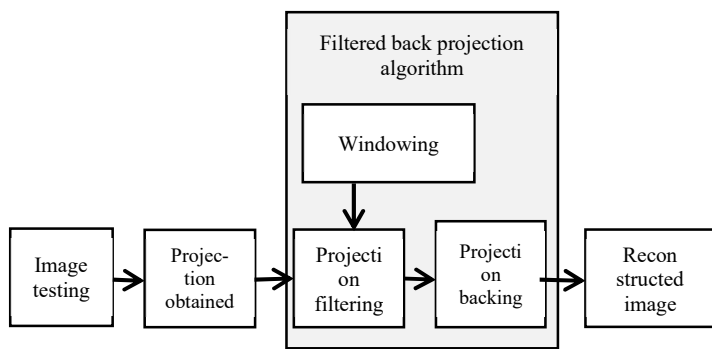


Figure 2. System reconstruction block diagram

**V. RESULTS**

The projection will receive an X-ray snapshot while scanning the object at the theta angle after applying computer simulations of FBP to the image. Examples of the many variables that affect the performance and image quality of the method include image size, the number of projections, and incremental.

The genotype is a series of parallel projections taken at equidistant angles of the object, providing a map of the projection data [16, 25], and the data gathered may be represented as a two-dimensional sinogram. The input image pocket diagram is shown in Figure 3:

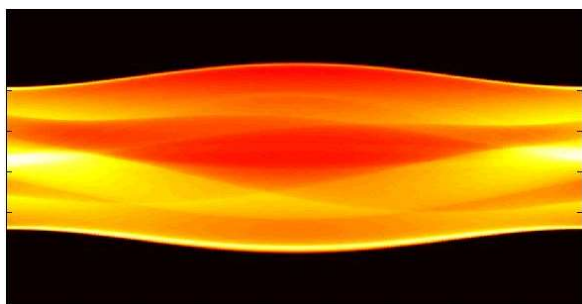


Figure 3. The input image sinogram

After applying the aforementioned sinogram in theta in the range (0: 179) with the step size, the step size effect 1 shows the image quality. Figure 4 depicts a Sinogram with a 10° step size.

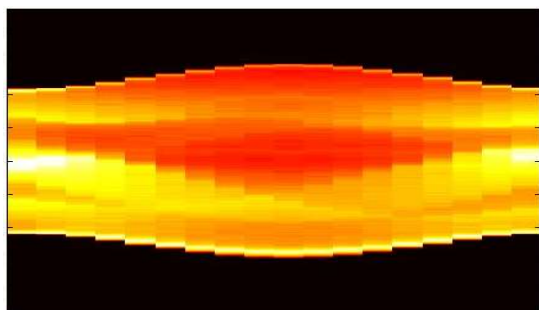


Figure 4. The Sinogram with a step size of 10 degrees

The X-ray detectors will identify each projection in the same way under both conditions. The reconstructed images are shown at different  $\Delta t$  in Figure 5:

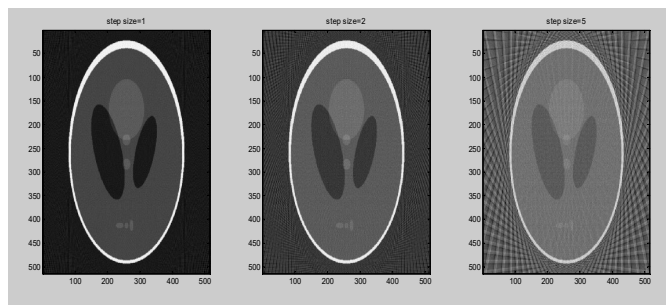


Figure 5. The numerous reconstructions of the  $\Delta t$

Figure 6 illustrates the anticipated reconstruction time for each scenario of  $\Delta t$  as well as the correlation between the step size and image size and performance.

The impact of the  $\Delta t$  parameter on the expected duration of the reconstruction process and performance is evident in the plot diagram above. The  $\Delta t$  parameter is crucial to the quality of the reconstructed pictures because of these reciprocal interactions. Picture size may be in the vertices of these parameters, which are necessary to address this problem in order to minimize computations and maintain the quality of the reconstructed picture. Table 2 provides the influence of picture size parameter for the three scenarios displayed in Figure 6.

Using the Ram-Lak filter, each of predictions will be given a weight. To avoid the fuzzy picture later known as the Ram-Lak filter (10), the slope filter will be struck by the Hanning window, which will double both filters and reduce the impact of noise at high image frequencies. Figure 7 shows the Ram-Lak filter and the Hann window.

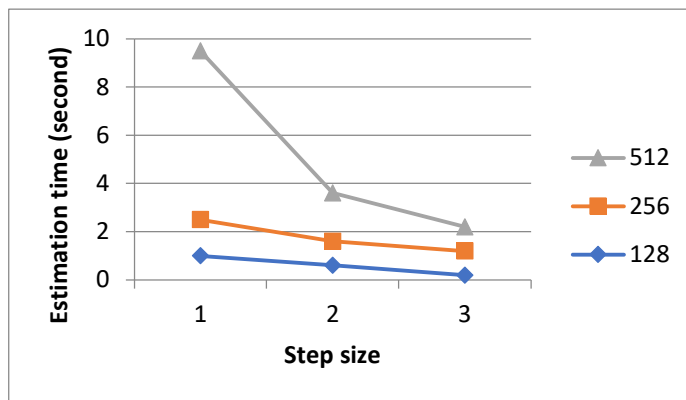


Figure 6. The estimated time of reconstruction diagram

**Table 2. The effect of step size ( $\Delta t$ ) and image size on the reconstruction performance**

	Image size (pixel)	Estimated time (sec)		
		$\Delta t=1$	$\Delta t=2$	$\Delta t=5$
Case 1	512x512	9.6877	4.6644	1.8408
Case 2	256x256	2.3712	1.2324	0.4524
Case 3	128x128	0.6084	0.3120	0.1872

Equation (11) may be utilized to recreate the object by employing these filtered projections. The output of the FBP algorithm for the CT scanner test picture in Figure 3 is given in Figure 8.

Figure 9 shows an image reconstruction with Sinogram in Figure 4. Sinogram will give some indications about the reconstructed image.

To use high-level language, we get the estimated time of less than 10 seconds to reconstruct the image of 512 x 512 pixels.

In the Ram-Lake filter, the ramp filter will be multiplied by the sinc function. The spatial impulse responses and transfer functions of the applied Ram-Lake filters are displayed in Figures 3a and 3b, respectively.

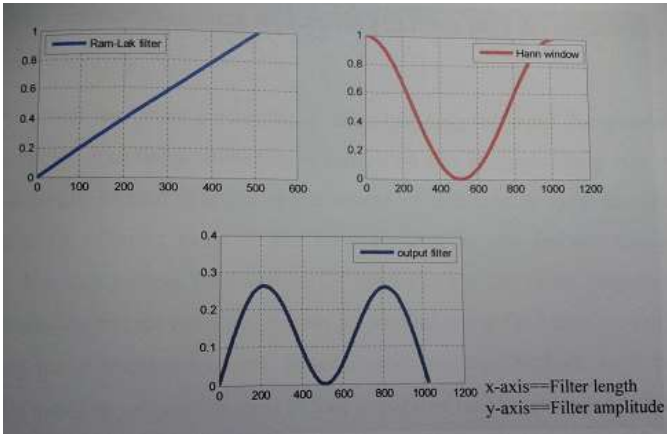


Figure 7. The Ram-Lake filter diagrams

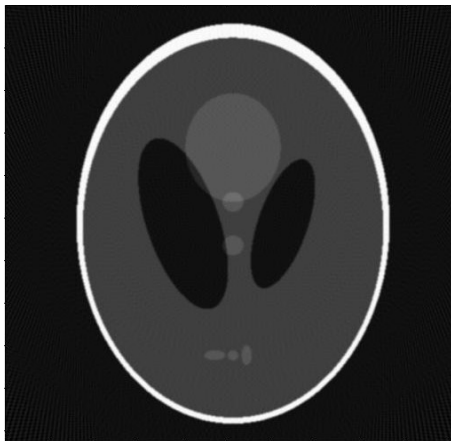


Figure 8. Reconstructed image



Figure 9. Image reconstruction with sonogram

It is determined due to the experiments that there is an equal number of sensing detectors for each projection, and the raw data matrix will be large enough to define the number of

detectors detecting and the attenuation coefficient for each projection. Apply the FBP method to each slice to rebuild it before taking another one once the data has been gathered from each projection using the Radon transform. Every projection will have a distinct set of raw data. The projection is displayed at certain angles of 1, 90, and 180, respectively, in Figure 10, Figure 11, and Figure 12. When the number of projections increases, the slight discrepancy between the initial and rebuilt projections will vanish. The impact of employing various forecasts will be ascertained using RMSE (Root Mean Square Error) values. The bar graph of the RMSE value as the number of projections varies is displayed in Figure 13.

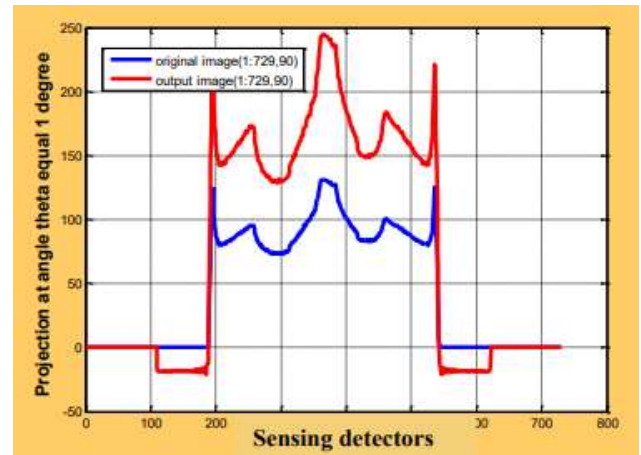


Figure 10. The projection data at theta equal to 1 degree

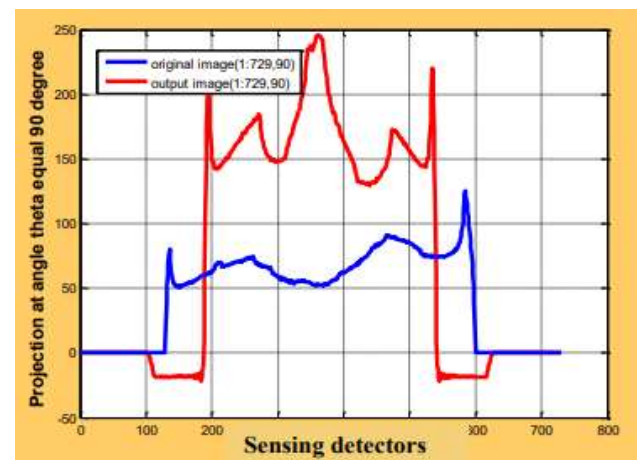


Figure 11. The projection data at theta equal to 90 degrees

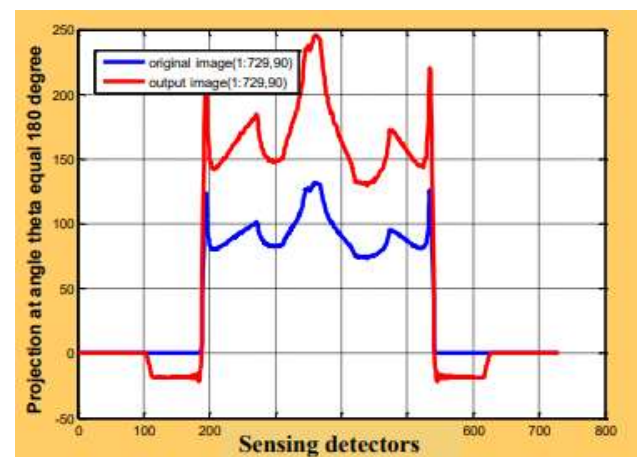


Figure 12. The projection data at theta equal to 180 degrees

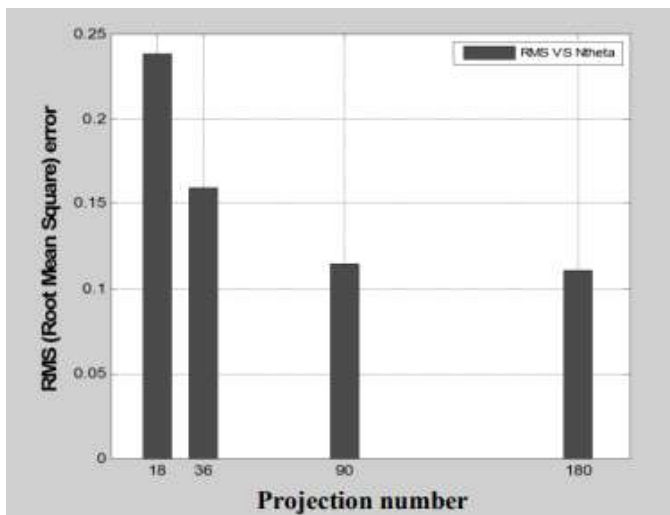


Figure 13. The relationship between the RMSE and the projection number

## VI. DISCUSSION

The reconstruction process is applied to CT scans by means of a filtered back projection technique for image optimization, followed by projection recombination to produce the rebuilt image. CT is widely used in biological applications and diagnostics because it can correctly represent anatomical features like bones and organs and can pick slides in any orientation. It also provides excellent contrast between soft tissues and spatial detail.

This is consistent with what researchers Marwa T. Al Hussani and Mohammed H. Ali Al Hayani (2014) mentioned, as they captured filtered back projection by capturing slices in different directions.

Theta angle increments are specified to be  $10^\circ$  in the interval  $[0^\circ-180^\circ]$  for each projection's X-ray detectors, which were employed in the same manner in all scenarios. In Tuğba Özge Onur's study (2021), the theta angle increments were  $5^\circ$  within the interval  $[0^\circ-180^\circ]$ .

Equation 1 illustrates the back projection approach that was presented by Ramachandran and Lakshminarayanan in 1971. The Hanning window multiplies the slope filter, doubling both filters and lowering the noise effect at high picture frequencies. The Ram-Lac filter and the Hahn window can be seen in Figure 7. This is what was used in the current study to rebuild high-resolution images while accounting for the three factors that affect reconstruction: picture size, number of projections, and incremental.

## VII. CONCLUSIONS

A useful and effective method for reconstructions in CT scanning data is the FBP algorithm. In medical applications, reconstructions are especially important since the patient has to be exposed to radiation as little as possible, which may need an additional slice. What is to be done right away following the first slide? The use of several filters to reduce back projection computations is the reason for the expected pressure on reconstruction time. The effect that these filters have is also very important in obtaining a satisfactory quality of image after reconstruction. The results for both filters were obtained using the Hann window and the Ram-Lak filter. On the selected photographs, the Hann filter was consistently found to perform better than the other filters. It is crucial to ascertain the

advantage of the FBP algorithm because the time needed is reduced by three times when compared to other algorithms.

## References

- [1] M. J. Willemink and P. B. Noël, "The evaluation of image reconstruction for CT-from filtered back projection to artificial intelligence," *Eur. Radiol.*, vol. 29, pp. 2185–2195, 2019. <https://doi.org/10.1007/s00330-018-5810-7>.
- [2] J. Hsieh, *Computed Tomography: Principles, Design, Artifacts, and Recent Advances*, 2nd ed, Wiley, 2009.
- [3] L. W. Goldman, "Principles of CT and CT Technology," *Journal of Nuclear Medicine Technology*, vol. 35, pp. 115-128, 2007. <https://doi.org/10.2967/jnmt.107.042978>.
- [4] Z. Qiao, G. Redler, B. Epel, and H. J. Halpern, "Comparison of parabolic filtration methods for 3D filtered back projection in pulsed EPR imaging," *J. Magn. Reson.*, vol. 248, pp. 42–53, 2014. <https://doi.org/10.1016/j.jmr.2014.08.010>.
- [5] J. B. T. M. Roerdink, M. A. Westenberg, "Data-parallel tomographic reconstruction: A comparison of filtered backprojection and direct Fourier reconstruction," *Parallel Computing*, vol. 24, pp. 2129-2142, 1998. [https://doi.org/10.1016/S0167-8191\(98\)00095-7](https://doi.org/10.1016/S0167-8191(98)00095-7).
- [6] S. Basu, Y. O. Bresler, "(N/sup 2/log/sub 2/N) filtered backprojection reconstruction algorithm for tomography," *IEEE Trans. Image Process.*, vol. pp. 1760–1773, 2000. <https://doi.org/10.1109/83.869187>.
- [7] T. Pipatsrisawat, A. Gacic, F. Franchetti, M. Puschel and J. M. F. Moura, "Performance analysis of the filtered backprojection image reconstruction algorithms," Proceedings of the 2005 IEEE International Conference on Acoustics, Speech, and Signal Processing, ICASSP'05, Philadelphia, March 18-23, 2005, pp. 153-156, <https://doi.org/10.1109/ICASSP.2005.1416263>.
- [8] M. T. Al Hussani, M. H. Ali Al Hayani, "The use of filtered back projection algorithm for reconstruction of tomographic image," *Al-Nahrain University, College of Engineering Journal (NUCEJ)*, vol. 17, no.2, pp.151-156, 2014.
- [9] N. Koshev, E. S. Helou, E. X. Miqueles, *Fast Backprojection Techniques for High Resolution Tomography*, arXiv:1608.03589v1, 2016.
- [10] T. Ö. Onur, "An application of filtered back projection method for computed tomography images," *International Review of Applied Sciences and Engineering*, vol. 12, issue 2, pp. 194-200, 2021. <https://doi.org/10.1556/1848.2021.00231>.
- [11] K. Cho, J. Chae, R.-Y. Kwon, S.-C. Bong, K.-S. Cho, "The application of the filtered backprojection algorithm to solar rotational tomography," *The Astrophysical Journal*, vol.895, no. 1, pp. 1-12, 2020. <https://doi.org/10.3847/1538-4357/ab88af>.
- [12] W. R. Hendee, E. R. Ritenour, *Medical Imaging Physics*, John Wiley & Sons, Inc., 2002. <https://doi.org/10.1002/0471221155>.
- [13] D. M. Pelt, V. De Andrade, "Improved tomographic reconstruction of large-scale real-world data by filter optimization," *Adv Struct Chem Imag.*, vol. 2, article id: 17, 2016. <https://doi.org/10.1186/s40679-016-0033-y>.
- [14] G. T. Herman, *Fundamentals of Computerized Tomography: Image Reconstruction from Projections*, second edition, Springer, 2009.
- [15] D. F. G. de Azevedo, S. Helegda, P. C. Godoy, F. de Castro and M. C. de Castro, "Tomography simulation and reconstruction tools applied in the evaluation of parameters and techniques," *Proceedings of the 2001 Conference Proceedings of the 23rd Annual International Conference of the IEEE Engineering in Medicine and Biology Society*, 2001, vol. 3, pp. 2260-2263, <https://doi.org/10.1109/IEMBS.2001.1017224>.
- [16] A. V. Oppenheim, and R. W. Schaffer, *Discrete-Time Signal Processing*, Prentice-Hall, pp. 447-448, 1989.
- [17] S. A. Qureshi, S. M. Mirza and M. Arif, "Inverse radon transform-based image reconstruction using various frequency domain filters in parallel beam transmission tomography," *Proceedings of the 2005 IEEE Student Conference on Engineering Sciences and Technology*, Karachi, Pakistan, 2005, pp. 1-8. <https://doi.org/10.1109/SCONEST.2005.4382887>.
- [18] X. Li, Y. He, Q. Hua, "Application of computed tomographic image reconstruction algorithms based on filtered back-projection in diagnosis of bone trauma diseases," *Journal of Medical Imaging and Health Informatics*, vol. 10, no. 5, pp. 1219-1224, 2020. <https://doi.org/10.1166/jmhi.2020.3036>.
- [19] P. Prabhat, S. Arumugam, V. K. Madan, "Filtering in filtered backprojection computerized tomography," *Proceedings of the National Conference "NCNTE-2012" at Fr. C.R.I.T., Vashi, Navi Mumbai*, Feb. 24-25, 2012.

- [20] D. M. Pelt, K. J. Batenburg, "Accurately approximating algebraic tomographic reconstruction by filtered backprojection," *Proceedings of the 13th International Meeting on Fully Three-Dimensional Image Reconstruction in Radiology and Nuclear Medicine*, 2015, pp. 158–161.
- [21] R. Kumar, S. Hans, "Filtered back projection algorithm on computed tomography (CT) scan," *International Research Journal of Engineering and Technology*, vol. 3, issue 6, pp. 2152-2156, 2016.
- [22] Z. Wang, J. Cai, W. Guo, M. Donnelly, D. Parsons, I. Lee, "Backprojection wiener deconvolution for computed tomographic reconstruction," *PLoS ONE*, 13(12): e0207907, 2018. <https://doi.org/10.1371/journal.pone.0207907>.
- [23] L. Raczynski, W. Wiślicki, and et al, "Introduction of total variation regularization into filtered backprojection algorithm," *Acta Physica Polonica B*, vol. 48, no. 10, pp. 1611-1618, 2017. <https://doi.org/10.5506/APhysPolB.48.1611>.
- [24] R. Maitra, "Efficient bandwidth estimation in 2D filtered backprojection reconstruction," *IEEE Transactions on Image Processing*, vol. 28, no. 11, pp. 5610-5619, 2019, <https://doi.org/10.1109/TIP.2019.2919428>.
- [25] M. Andrew, B. Hornberger, *Iterative Reconstruction for Optimized Tomographic Imaging*, ZEISS Microscopy, Germany, 2018.



**FAIEZ MUSA LAHMOOD ALRUFAYE** received a master's degree in computer science from the University of Basra in southern Iraq. He is currently working at the Middle Technical University as a lecturer. He published 8 research papers in international journals with high impact factor. ORCID: <https://orcid.org/0000-0002-0396-3916>



**SEHAM AHMED HASHEM** received her BSc, MSc and PhD from University of Technology, Baghdad. Currently she is full time Ass. Prof. in Middle Technical University. She has been a senior researcher in a center of Iraqi development since 1986. She has good skills in the design and modelling of Soft Computing system and image processing and communication. She published more than 30 research works and participated in many international conferences. ORCID: <https://orcid.org/0000-0002-0506-1684>

...